The electromechanical damping of piezo actuator resonances

Theory and practice

van Spengen, W. Merlijn

DOI
10.1016/j.sna.2021.113300

Publication date
2022

Document Version
Final published version

Published in
Sensors and Actuators A: Physical

Sensors and Actuators: A. Physical 333 (2022) 113300

Contents lists available at ScienceDirect

Sensors and Actuators: A. Physical

journal homepage: www.elsevier.com/locate/sna

The electromechanical damping of piezo actuator resonances: Theory and practice

W. Merlijn van Spengen[a,b]

[a] Falco Systems, Remisestraat 1, 2225TH Katwijk aan Zee, The Netherlands
[b] Delft University of Technology, 3mE-PME-MNE, Mekelweg 2, 2628CD Delft, The Netherlands

ARTICLE INFO

Article history:
Received 9 August 2021
Received in revised form 2 November 2021
Accepted 2 December 2021
Available online 5 December 2021

Keywords:
Piezoelectric actuator
Resonance
Optimal damping
Electronic model

ABSTRACT

Piezo actuators have very desirable properties, such as a high stiffness and extreme position resolution, but suffer from electromechanical resonances that complicate their use in high-speed applications. These resonances can be minimized by using resistive or resistive-inductive damping.

In this paper a comprehensive theory is presented which describes these piezo resonances, and the mechanism by which these resonances are minimized by adding electrical damping components. The theory is based on a purely electronic model, and uses an electrical-mechanical transformation to describe actual piezo displacements. Using this theory, an 'optimal' value of damping resistance is readily identified. This optimal resistance causes maximal damping of the primary resonance of the piezo. It is shown that damping with a combination of a resistor and an inductor can theoretically be even better.

An optical displacement setup was developed, and frequency- and time-domain measurements were performed that validate the theory. The mechanical damping of the piezo actuator needs to be included in the theory to obtain a good fit with the electrical and mechanical behavior of an actual piezo actuator.

1. Introduction

Piezoelectric crystal actuators (piezos in short) are used in many precision positioning applications. They provide a high stiffness, high force, and a high maximum operating frequency, while at the same time allowing for a very high positioning resolution. Compared to most other actuators, their stroke (maximum displacement) is relatively low. Despite their excellent properties, it is difficult to use piezos in high-speed applications, because they suffer from large electromechanical resonances [1]. In the current paper a comprehensive theory of electronic damping of piezo actuator resonances using R- (resistor) and RL-(resistor-inductor) compensation is presented in purely electronic terms. This theory allows the calculation of the mechanical response of the piezo and optimal damping component values. It is validated by a comparison of the predictions of the theory and corresponding experiments.

Early work on driving piezos electrically came from the radio engineering community, which uses piezos to stabilize the frequency of oscillators. For a frequency-stable oscillator, damping should be minimized, and the resultant quality factor Q of the piezo should be as high as possible [2]. The need to actually damp piezo actuator resonances instead of enhancing the Q came with their use as precision actuators and in passive damping systems. Most of the public literature is concerned with piezos used as passive dampers for vibration isolation, not with piezos used primarily for actuation. For an overview of passive piezo damping options, see Moheimani and Fleming [3]. Seen from a systems point of view, the two are very similar. The resistive and resistive-inductive compensation techniques discussed in the current paper are common to both.

The material science and mechanical properties of piezos are well-known, see e.g. Moulson and Herbert [4]. In comparison, relatively little literature is available dealing exclusively with the electronic properties of piezos. A piezo has many higher harmonic resonances modes [5,6], but in most cases only the 'fundamental' resonance is taken into account, because it is usually the strongest one. The electromechanical modeling of piezo actuators started with the derivation of the Butterworth–van Dyke electrical model of the fundamental resonance of a piezo, which was devised in the 1920s [7].

Several versions of this model were used to describe the properties of piezos, see e.g. Stutts [8], Queiros et al. [9], Fernandez-Afonso et al. [10] and Sriratana et al. [11]. Prokic [12] presents the effect of a damping series resistor in graphical form. He also recognizes the importance of the 'mechanical current', discussed in Section 2, as a measure for the piezo velocity. Thomas et al. [13]

E-mail address: vspengen@falco-systems.com.

https://doi.org/10.1016/j.sna.2021.113300
0924-4247/

address the passive reduction of structural vibration by means of shunted piezoelectric patches in great depth. Contrary to the approach followed in the current paper, they mathematically follow a mechanical resonance framework instead of the electronic description presented here. Even though they do not consider piezos for actuation, only for passive damping, they obtain equations describing important features of piezo damping, such as peak shift, quality factor reduction, and the 'saddle' that is characteristic of resistor-inductor compensation.

The current paper fills the gap between the passive-mechanical approach in the literature, and the less comprehensive electronic treatments of piezo actuators to date. It also serves as the background to choose an optimal electronic damping strategy for actual experiments that include a piezo actuator. We start with a description of the piezo connected directly to a low impedance 'hard' voltage source piezo driver. It is shown that this results in a high, sharp mechanical resonance peak. It is much better to connect the piezo to its driver via a suitable coupling network, consisting of either a resistor, or a resistor and an inductor. A 'midpoint' resistor value for highest damping can be derived, and it is shown that combining it with a properly chosen inductor is even better theoretically. The theoretical results are compared to experimentally obtained data on an actual piezo actuator and shown to be in excellent agreement both electrically and mechanically. This allows the users of piezo actuators to obtain an optimized damped response using a simple procedure.

2. The Butterworth–van Dyke model and the theory of the resistively coupled piezo without mechanical damping

The Butterworth–van Dyke electrical model of a piezo [7] in Fig. 1 is an example of a coupled electromechanical system. The mechanical behavior of the mass-spring system (corresponding to the piezo with mass, stiffness and damping) causes an electrical effect modeled by an inductance L_m, a capacitance C_m, and a resistive damping term R_m. These are coupled to the electrical capacitance C_o of the piezo, which can be measured between the electrodes at frequencies which are low compared to the resonance frequency. The combined electromechanical system is not a standard second order system due to the coupling with C_o.

The current i_{mech} that flows through the series impedance of R_m, L_m, and C_m is a direct measure of the velocity u of the piezo actuator [12]. Knowing the electrical circuit parameters, we can calculate the velocity response u of the piezo element to a driving voltage v and current i, and hence also the displacement amplitude d, because the displacement is the integral over time of the velocity, $d = \int u dt$. Therefore, we have the possibility to model the mechanical response of the piezo as a purely electronic phenomenon, and afterwards derive the mechanical response by assessing i_{mech}. Van Dyke [7] arrives at the model of Fig. 1 by considering that the equivalent mechanical current is related to the velocity of the piezo. An alternative derivation of the Butterworth–van Dyke electrical model of a piezo is given in [14].

In the current paper, we will use increasingly more complex electrical models of the piezo and its drive circuitry to describe the mechanical response of the piezo system to an electrical voltage stimulus using the i_{mech} concept. More elaborate electronic models than the Butterworth–van Dyke model have also been proposed [15],

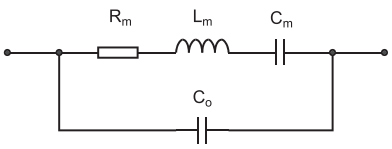

Fig. 1. Butterworth–van Dyke equivalent schematic of a piezo actuator.

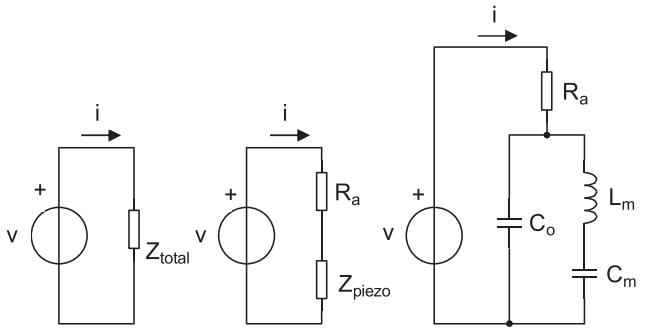

Fig. 2. Equivalent circuits of the voltage source driven piezo with added series resistance R_a.

but it will be shown in the experimental Sections 6 and 7 that they are not needed for an accurate understanding of the behavior of a typical piezo actuator. Verbiest et al. [16] have also shown that using the Butterworth–van Dyke model results in a very good fit of the measured piezo primary resonance.

In a typical setup a piezo actuator is driven by a voltage source with output voltage v. This voltage source can be e.g. the output of a high voltage amplifier (often also called "piezo driver"). Usually the piezo is directly connected to the output of the amplifier, effectively creating a piezo system directly driven from a 'hard' voltage source. But to minimize mechanical resonances it is much better to use a resistance R_a in series with the piezo [3]. In the following theoretical section, it will be shown, using the electronic model, why this is the case.

We start with the simplest model of the system that displays the required behavior, to keep the algebra tractable. In Fig. 2, the electrical model of the piezo with series resistance R_a is shown. The mechanical damping resistor R_m of Fig. 1 is assumed here to be negligibly small, so it has been omitted from this first model. Its effect will be calculated later in the paper. The impedance Z_{mech} of the mechanical branch of the piezo is the series impedance of L_m and C_m

$$Z_{mech} = j\omega L_m + \frac{1}{j\omega C_m} = \frac{1-\omega^2 C_m L_m}{j\omega C_m} \tag{1}$$

The impedance of the piezo, including C_o, is the parallel circuit of Z_{mech} and C_o, calculated as

$$Z_{piezo} = Z_{mech}//Z_{C_o} = \frac{Z_{mech}Z_{C_o}}{Z_{mech}+Z_{C_o}} = \frac{1-\omega^2 C_m L_m}{j\omega(C_o + C_m - \omega^2 C_o C_m L_m)} \tag{2}$$

The total impedance Z_{total} seen by the voltage source is the impedance of the piezo Z_{piezo} and the resistor R_a in series, given by

$$Z_{total} = Z_{piezo} + R_a = \frac{1-\omega^2 C_m L_m + j\omega R_a(C_m + C_o - \omega^2 C_m C_o L_m)}{j\omega(C_o + C_m - \omega^2 C_o C_m L_m)} \tag{3}$$

As a result, a current i will flow through Z_{total} in response to a voltage source with output voltage v, given by Ohms law as

$$i = \frac{v}{Z_{total}} = \frac{j\omega(C_o + C_m - \omega^2 C_o C_m L_m)}{1-\omega^2 C_m L_m + j\omega R_a(C_m + C_o - \omega^2 C_m C_o L_m)} \cdot v \tag{4}$$

We obtain the physical, real current with magnitude $|i|$, which can actually be measured, from the complex current by taking the square root of the complex current times its complex conjugate. This corresponds to the length of the current vector in the complex plane, and is

$$|i| = \sqrt{\frac{\omega^2(C_o + C_m - \omega^2 C_o C_m L_m)^2}{(1-\omega^2 C_m L_m)^2 + \omega^2 R_a^2 (C_m + C_o - \omega^2 C_m C_o L_m)^2}} \cdot v \tag{5}$$

Using the complex current i and the impedance Z_{piezo} of the piezo, the voltage v_{piezo} across the piezo is calculated, again with Ohms law, as

$$v_{piezo} = i \cdot Z_{piezo} = \frac{j\omega(C_o + C_m - \omega^2 C_o C_m L_m)}{1 - \omega^2 C_m L_m + j\omega R_a(C_m + C_o - \omega^2 C_m C_o L_m)} \cdot \frac{1 - \omega^2 C_m L_m}{j\omega(C_o + C_m - \omega^2 C_o C_m L_m)} \cdot v$$

$$= \frac{1 - \omega^2 C_m L_m}{1 - \omega^2 C_m L_m + j\omega R_a(C_m + C_o - \omega^2 C_m C_o L_m)} \cdot v \quad (6)$$

The corresponding magnitude of the physical voltage across the piezo that can be actually measured, is again obtained by taking the square root of the complex current times its complex conjugate

$$|v_{piezo}| = \sqrt{\frac{(1 - \omega^2 C_m L_m)^2}{(1 - \omega^2 C_m L_m)^2 + \omega^2 R_a^2 (C_m + C_o - \omega^2 C_m C_o L_m)^2}} \cdot v \quad (7)$$

The voltage v_{piezo} across the piezo is directly across the mechanical branch Z_{mech} in the piezo model, and the 'mechanical' current i_{mech} flowing through this branch can be calculated using Ohms law as well,

$$i_{mech} = \frac{v_{piezo}}{Z_{mech}} = \frac{1 - \omega^2 C_m L_m}{1 - \omega^2 C_m L_m + j\omega R_a(C_m + C_o - \omega^2 C_m C_o L_m)} \cdot \frac{j\omega C_m}{1 - \omega^2 C_m L_m} \cdot v$$

$$= \frac{j\omega C_m}{1 - \omega^2 C_m L_m + j\omega R_a(C_m + C_o - \omega^2 C_m C_o L_m)} \cdot v \quad (8)$$

The corresponding magnitude of the mechanical current is

$$|i_{mech}| = \sqrt{\frac{\omega^2 C_m^2}{(1 - \omega^2 C_m L_m)^2 + \omega^2 R_a^2 (C_m + C_o - \omega^2 C_m C_o L_m)^2}} \cdot v \quad (9)$$

In the Butterworth–van Dyke model, the magnitude of the mechanical current $|i_{mech}|$ thus obtained is linearly related to the magnitude of the velocity $|u|$ of the piezo. The displacement d of the piezo is the integral $d = \int u dt$ of the velocity u with respect to time t for every conceivable velocity u. If we assume the piezo velocity to be $u = \cos(\omega t)$, the displacement is

$$d = \int \cos(\omega t) dt = \frac{1}{\omega} \sin(\omega t) \quad (10)$$

As there is a linear relation between the magnitude of the mechanical current $|i_{mech}|$ and the magnitude of the velocity $|u|$, Eq. (10) means that there must also be a linear relation between $|i_{mech}|/\omega$ and the displacement magnitude $|d|$, which can be said, without loss of generality, to be linked by a proportionality constant α:

$$|d| = \frac{\alpha}{\omega} \cdot |i_{mech}| = \frac{\alpha}{\omega} \sqrt{\frac{\omega^2 C_m^2}{(1 - \omega^2 C_m L_m)^2 + \omega^2 R_a^2 (C_m + C_o - \omega^2 C_m C_o L_m)^2}} \cdot v$$

$$= \alpha C_m \sqrt{\frac{1}{(1 - \omega^2 C_m L_m)^2 + \omega^2 R_a^2 (C_m + C_o - \omega^2 C_m C_o L_m)^2}} \cdot v \quad (11)$$

The value of the proportionality constant α is obtained by assessing the piezo displacement to an actuation voltage for $\omega \to 0$, the static displacement to an actuation voltage. This property of a piezo is given by the manufacturer as the 'piezo travel' or sensitivity, typically in µm/V. If we evaluate the equation for $|d|$ given above for $\omega \to 0$, we obtain

$$|d| = \alpha C_m \cdot v \quad (12)$$

which shows that the proportionality constant α corresponds to the piezo travel, divided by the mechanical capacitance C_m.

Table 1
Fitted P-820.20 piezo model parameters.

Component	*Value*
C_m	19.2 nF
L_m	0.50 mH
R_m	2.5 Ω
C_o	0.48 µF

To present the theory above in figures, numbers need to be inserted in the respective equations. The values used were obtained by fitting the theory to the experimentally obtained results as discussed in Section 6. For these experiments, the Physik Instrumente P-820.20 piezo was used. These experimentally obtained values corresponding to the Butterworth–van Dyke model are given in Table 1.

Using the values given in Table 1, but with $R_m = 0$, the theory presented above is illustrated in Figs. 3–6. For calibrating the piezo displacement given in Fig. 6 the fact is used that the static sensitivity of the piezo is given by the manufacturer as 0.3 µm/V ± 20% [17].

It can be seen that when the piezo is driven by a hard voltage source ($R_a = 0\,\Omega$), the current drawn by the piezo first goes through a maximum. This maximum is at the 'primary resonance frequency' of the piezo. This is the purely mechanical resonance defined by C_m and L_m. At the primary resonance, the mechanical current and hence the velocity and displacement magnitude of the piezo are very high and only limited by the mechanical damping resistance R_m. Driving the piezo at this frequency without an added series resistance highly stresses both the piezo actuator and the high voltage amplifier driving it. At a somewhat higher frequency, the parallel 'anti-

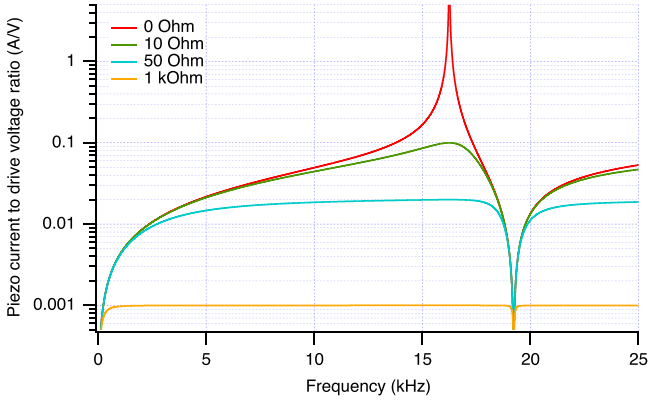

Fig. 3. Theoretical current $|i|$ through R_a and Z_{piezo} in series; no mechanical damping R_m.

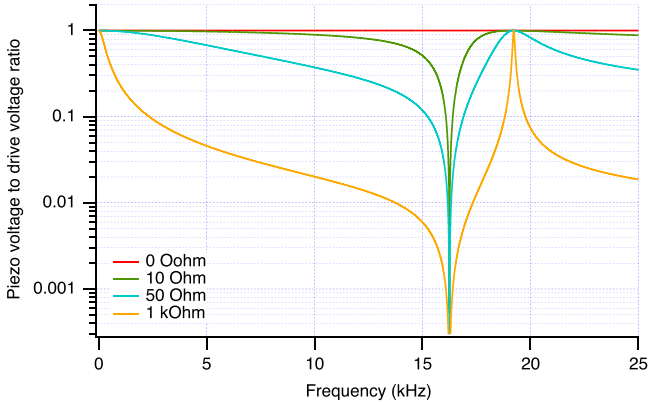

Fig. 4. Theoretical voltage $|v|$ over the piezo, modeled by Z_{piezo}; no mechanical damping R_m.

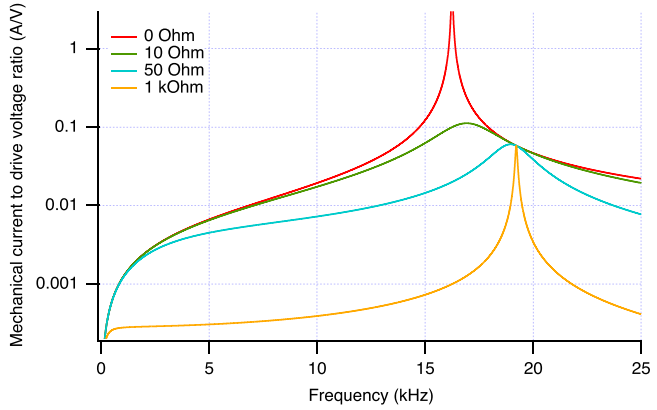

Fig. 5. Theoretical current $|i_{mech}|$ through the mechanical piezo resonator Z_{mech}; no mechanical damping R_m.

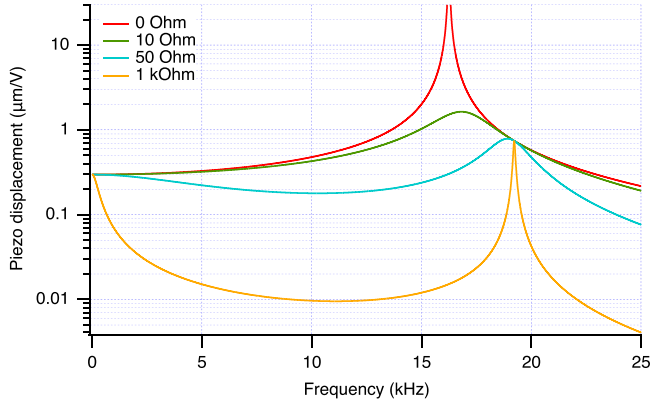

Fig. 6. Theoretical piezo displacement $|d|$; no mechanical damping R_m.

resonance' is visible, where C_m, L_m and C_o all play a role. At this frequency, no extra current is drawn by the piezo when $R_a = 0\,\Omega$. In this case, there is no extra mechanical current, and hence no mechanical resonance is present at the anti-resonance frequency.

When the series resistance $R_a \neq 0$, the voltage across the piezo is not constant, and the voltage v_{piezo} over the piezo will start to gradually decrease with increasing frequency due to the low-pass filter formed by R_a and C_o. But near the primary resonance it will drop further, because the extra current drawn by the piezo resonance creates an extra voltage drop across R_a. As a result, the full voltage is no longer available to drive the primary resonance. The net effect is a lowering the peak of the primary resonance visible in the mechanical current and displacement curves, and a shift of this lowered primary resonance peak to a higher frequency.

As R_a continues to increase, the drive to the piezo becomes progressively more similar to a current source. Now only at the anti-resonance there is a significant voltage across the piezo. The mechanical current $|i_{mech}|$ will have a maximum at the anti-resonance frequency, with an amplitude defined by the envelope of the primary resonance curve for $R_a = 0$. This is also true for the displacement $|d|$ of the piezo at the anti-resonance frequency.

Both very low and very high R_a values will give rise to a sharp mechanical resonance, at the electrical resonance and anti-resonance frequencies respectively. The amplitude of the mechanical resonance is lower at the electrical anti-resonance, but as we have seen the resonance still has a high quality factor Q. Between them, there is an R_a for which maximum damping is obtained. To use a piezo actuator with a mechanical resonance as low as possible, driving it with a voltage source including series resistance R_a close to the value required for maximum damping is highly desirable. As shown in Appendix A, the value of this specific R_a, which we will call $R_{a,mid}$, is

$$R_{a,mid} = 2\sqrt{\frac{C_m L_m}{C_o(4C_o + C_m)}} \tag{13}$$

The value of $R_{a,mid}$ is not significantly affected by the size of the piezo. As C_m, L_m, and C_o all three change by roughly the same factor when a piezo is made smaller or larger, the ratio given for $R_{a,mid}$ will remain the same. This means the optimal $R_{a,mid}$ has, to first order, a similar value for all sizes of piezo actuators made of the same material. Using the values of Table 1, its value evaluates to $R_{a,mid} \cong 20\,\Omega$ for PZT (Lead Zirconate Titanate) based piezo actuators such as the P-820.20 used for the experiments. Different piezo materials, such as quartz, will generally result in a different value for $R_{a,mid}$.

The addition of the piezo series resistance R_a results in a low-pass filtered response, determined by R_a and C_o. The question may arise whether separately low-pass filtering the drive signal may be just as effective as adding a damping resistor directly at the piezo, but this is not the case. A low-pass filter will lower the amplitude of both the resonance and the desired response, but will not change the quality factor Q of the resonance. It will also result in a lower amplitude of the resonance, but the resonance will not 'die out' as quickly as the resistively damped piezo response.

This can be seen as follows. A separate low pass filter with resistor R_f and capacitor C_f will at its output have a frequency-dependent voltage with magnitude $|v_f|$ that is lower than the drive voltage magnitude $|v|$ by

$$|v_f| = \frac{1}{\sqrt{1 + \omega^2 R_f^2 C_f^2}}\,|v| \tag{14}$$

In the case of a separate RC filter hence all that will happen is a reduction of the resonance amplitude and a phase lag, but the piezo resonance quality factor will not be affected. The response will still go (ideally) to infinity at the primary resonance, contrary to the case of resistive damping directly at the piezo. This important difference is shown experimentally in Section 8.

Control-based damping [18] is also described in literature to optimize the piezo response. Electronic damping as discussed in the current paper and control-based damping are complementary. A better damped physical system can be modeled better and will behave more like the model under varying circumstances, such as temperature changes. Hence the better the direct electronic damping, the easier it is to further compensate the resonance by control-based damping.

The addition of acoustic damping (e.g. by the inclusion of rubber-like materials in the mechanical loop) is beneficial to lower the piezo resonance amplitude also [3]. This increases the value or R_m, which lowers the resonance amplitude, as it lowers the current flowing between L_m and C_m, and between L_m and C_o. Acoustic damping is hence a complementary method to the electronic damping method presented in the current paper. Both acoustic and electronic damping can be combined to create a well-behaved system that can be further optimized by using control-based drive signals.

3. The theory of the resistively coupled piezo with mechanical damping

The theory presented until now suffices to understand in general terms what is happening in a system consisting of a piezo with series resistance R_a. It has also allowed us to calculate a recommended value of a series resistance that results in optimal damping of the electromechanical resonances of the piezo. However, if the theory as presented is fitted to the response of an actual piezo, it will be found that the resonances predicted for low and high R_a values are off by a

significant amount. Indeed, the electromechanical resonances of the piezo are not infinitely sharp, and for a good fit the model of the mechanical impedance Z_{mech} of the piezo needs to be modified to include the mechanical resistance R_m of the Butterworth–van Dyke model. This makes the algebra harder, but in principle the exact same procedure is followed. We now start with the mechanical impedance including mechanical damping, with subscript md, denoted $Z_{mech,md}$, as

$$Z_{mech,md} = R_m + j\omega L_m + \frac{1}{j\omega C_m} \tag{15}$$

Using the same steps as before, the following expressions are obtained with mechanical damping. We define the magnitude of the current $|i_{md}|$ which flows through R_a and the piezo, the magnitude of the voltage $|v_{piezo,md}|$ over the piezo, the magnitude of the mechanical current $|i_{mech,md}|$, and finally the mechanically damped piezo displacement magnitude $|d_{md}|$.

$$|i_{md}| = \sqrt{\frac{\omega^4 R_m^2 C_m^2 C_o^2 + \omega^2 (C_m + C_o - \omega^2 C_m C_o L_m)^2}{(1-\omega^2 C_m (L_m + R_a R_m C_o))^2 + \omega^2 (C_m (R_a + R_m) + R_a C_o - \omega^2 R_a C_m C_o L_m)^2}} \cdot v \tag{16}$$

$$|v_{piezo,md}| = \sqrt{\frac{(1-\omega^2 C_m L_m)^2 + \omega^2 R_m^2 C_m^2}{(1-\omega^2 C_m (R_a R_m C_o + L_m))^2 + \omega^2 (C_m (R_a + R_m) + R_a C_o - \omega^2 R_a C_m C_o L_m)^2}} \cdot v \tag{17}$$

$$|i_{mech,md}| = \sqrt{\frac{\omega^4 R_m^2 C_m^4 + \omega^2 C_m^2 (1-\omega^2 C_m L_m)^2}{\begin{array}{l}(1-\omega^2 (C_m (R_a R_m C_m + R_m^2 C_m + 2R_a R_m C_o + 2L_m \\ \quad - \omega^2 C_m (2R_a R_m C_o L_m + L_m^2))))^2 \\ + \omega^2 (C_m (R_a + 2R_m) + R_a C_o - \omega^2 C_m (R_a R_m^2 C_m C_o \\ \quad + R_a C_m L_m + 2R_m C_m L_m + 2R_a C_o L_m \\ \quad - \omega^2 R_a C_m C_o L_m^2))^2\end{array}}} \cdot v \tag{18}$$

$$|d_{md}| = \alpha C_m \sqrt{\frac{\omega^2 R_m^2 C_m^2 + (1-\omega^2 C_m L_m)^2}{\begin{array}{l}(1-\omega^2 (C_m (R_a R_m C_m + R_m^2 C_m + 2R_a R_m C_o + 2L_m \\ \quad - \omega^2 C_m (2R_a R_m C_o L_m + L_m^2))))^2 \\ + \omega^2 (C_m (R_a + 2R_m) + R_a C_o - \omega^2 C_m (R_a R_m^2 C_m C_o \\ \quad + R_a C_m L_m + 2R_m C_m L_m + 2R_a C_o L_m \\ \quad - \omega^2 R_a C_m C_o L_m^2))^2\end{array}}} \cdot v \tag{19}$$

It will be shown in Section 6 that these expanded equations, which include R_m, describe the actual piezo behavior with any value of series resistor extremely well. This is true both in the electronic and the mechanical domain.

4. The theory of the RL-coupled piezo with mechanical damping

Although a series resistor with value $R_{a,mid}$ minimizes the electromechanical resonance of the piezo, and places it midway between the primary resonance and the anti-resonance, it does not completely eliminate it. Therefore, sometimes a series inductor L_a is added to the series resistance, resulting in a configuration called RL-compensation [3], see Fig. 7. When the value of the inductor is chosen such, that $\omega_{mid} L_a \approx R_{a,mid}$, the remaining resonance peak of the piezo will be flattened further. Depending on the sharpness of the resonance, it will be either flattened as a whole, or a 'saddle'-shape will be created, where the piezo resonance is replaced by two resonances on either side of the original resonance frequency. However, it is easy to create resonances with RL-compensation that are actually larger than the already minimized resonance using $R_{a,mid}$ that one is trying to remove. This approach is therefore only to be recommended in situations where the electromechanical system is extensively studied and its properties well-known.

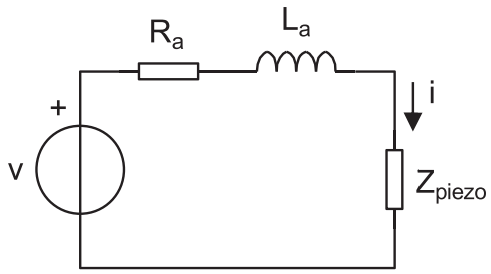

Fig. 7. The voltage source driven piezo with added series resistance R_a and series inductance L_a.

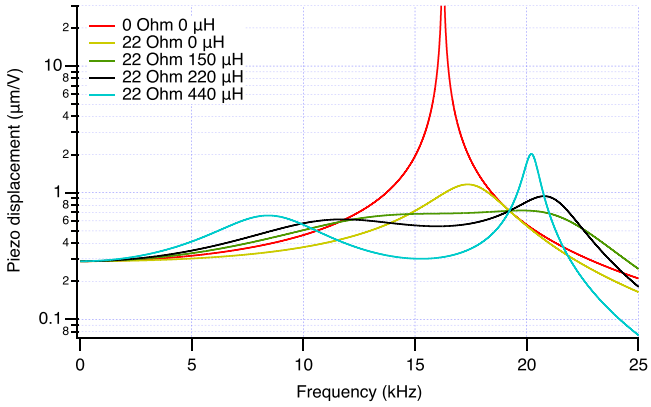

Fig. 8. Theoretical piezo displacement $|d_L|$ for RL-compensation, no mechanical damping R_m.

The same procedure followed previously can be employed to find the magnitude of the displacement including the series resistance R_a and now also the series inductance L_a. The total impedance seen by the voltage source is in the case of RL-compensation without R_m is

$$Z_{total,L} = R_a + j\omega L_a + Z_{piezo} \tag{20}$$

This results in a displacement $|d_L|$ with L_a present given by

$$|d_L| = \alpha C_m \sqrt{\frac{1}{(1-\omega^2 (C_m (L_a + L_m) + C_o L_a - \omega^2 C_m C_o L_a L_m))^2 + \omega^2 R_a^2 (C_m + C_o - \omega^2 C_m C_o L_m)^2}} \cdot v \tag{21}$$

When this equation is plotted as a function of the compensation inductance L_a, it is found that the highest damping is obtained if R_a is lowered somewhat with respect to its optimal value without L_a. In Fig. 8, we see there is an optimal value of L_a, where the resonance peak becomes 'maximally flat'. Beyond this value the resonance splits, and the curve obtains a saddle point. The sharpness of the two resonances thus obtained increase when L_a is increased further.

RL-compensation is highly sensitive to the exact value of L_a. In Fig. 8, we see the effect of tuning L_a over a relatively narrow range while keeping R_a constant. If L_a is too low, no beneficial effect will be observed, while if L_a is too large, the resulting resonances are worse than the resonance RL-compensation was supposed to solve.

For piezo actuators used at low frequencies, far below the mechanical resonance, the addition of both series resistance and inductance again results in a low-pass filtered response. As RL-compensation only works with low resistance values close to $R_{a,mid}$, its effect at frequencies far below the resonance of the piezo will usually be small.

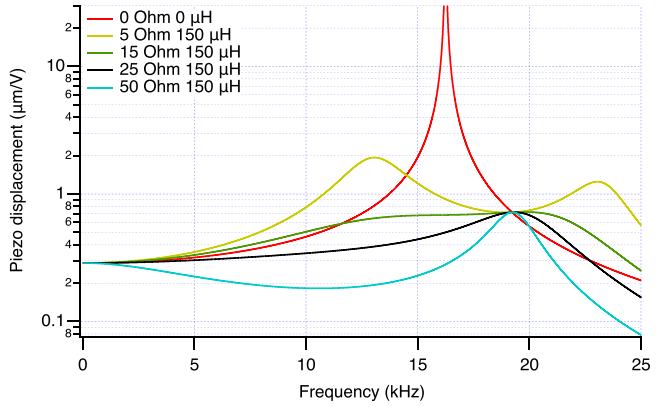

Fig. 9. The theoretical damping using RL-compensation is very sensitive to the exact value of the series resistance R_a.

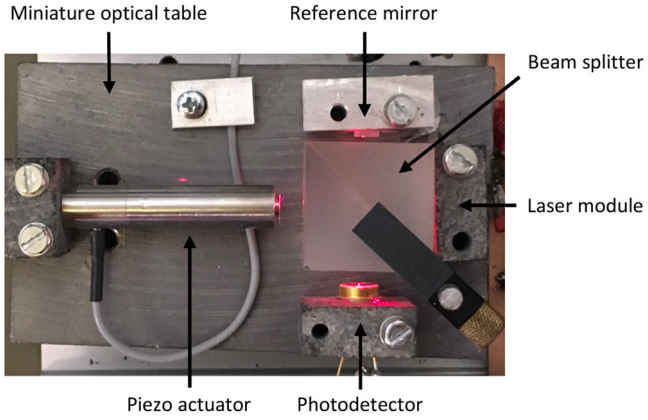

Fig. 10. Miniature optical table with interferometer to measure the piezo displacement curves.

As shown in Fig. 9, changing R_a in RL-damped scheme will result in a situation where there are two relatively large resonances if R_a is too small, and a case similar to resistive compensation alone if R_a is too high. This means that RL-compensation is much more sensitive to the exact component values, and hence also more sensitive to drift in the piezo parameters, than compensation with a series resistor R_a alone. The piezo properties are known to change with actuation voltage, temperature, and aging. In practice, it will be necessary to do a thorough assessment of parameter drift if this more advanced compensation is utilized. Otherwise, the further optimization with RL-compensation may in fact make matters worse under some operation conditions.

Without R_m the fit of this simple model to actual measured piezo data is again not perfect, because, at least for PZT based piezos, the optimal compensation resistance $R_{a,mid}$ is not orders of magnitude larger than the mechanical damping term R_m. The total impedance seen by the voltage source for RL-compensation including R_m is

$$Z_{total,md,L} = R_a + j\omega L_a + Z_{piezo,md} \tag{22}$$

Performing the same steps as before results in the following equation for the displacement $|d_{md,L}|$ with mechanical damping and RL-compensation introduced. Note that, compared to the situation with R_m but without L_a in Section 3, only the denominator has changed.

$$|d_{md,L}| = \alpha C_m \cdot \frac{\omega^2 R_m^2 C_m^2 + (1-\omega^2 C_m L_m)^2}{\sqrt{\begin{array}{l}(1-\omega^2(C_m(R_a R_m C_m + R_m^2 C_m + 2R_a R_m C_o + L_a + 2L_m) + C_o L_a \\ -\omega^2 C_m(R_m^2 C_m C_o L_a + 2R_a R_m C_m C_o L_m + C_m L_a L_m + C_m L_m^2 + 2C_o L_a L_m - \omega^2 C_m C_o L_a L_m^2))^2 \\ +\omega^2(C_m(R_a+2R_m)+R_a C_o \\ -\omega^2 C_m(C_m(R_a R_m^2 C_o + R_m L_a + L_m(R_a+2R_m)) \\ +2C_o(R_m L_a + R_a L_m) - \omega^2 C_m(2R_m C_o L_a L_m + R_a C_o L_m^2)))^2\end{array}}} \cdot v \tag{23}$$

5. Experimental setup

The theory presented above was verified with an in-house developed miniature optical detection setup. The whole setup is very compact to minimize the length of the mechanical loop [1] which in turn minimizes the parasitic mechanical resonances present in the system. Preliminary tests were performed with a proximity detector approach [19], using miniature optical tables made out of aluminum and granite and an optical mirror glued onto the piezo. But these experiments mainly showed parasitic mechanical resonances, and the proximity detector magnified the lateral bending motion of the piezo actuator, aggravated by the slightly off-axis mirror. Therefore, in the final version of the setup, which was used for the experiments reported on in this paper, a 10 × 6 × 4 cm solid block of lead (a very heavy and highly damping material), on rubber feet, was used as the optical table. The proximity detector was replaced by a miniature interferometer setup. To minimize the added mass and its associated axial asymmetry, only a partially reflective low mass piece of adhesive tape was glued onto the moving end of the piezo (Fig. 10). The laser diode module in the setup is a miniature 1 mW Picotronic DGI650-1-5(7 × 14)-F35-C125. This laser is meant to be used in pointing applications, such as the previously mentioned proximity sensor. It is not specified for interferometric applications, but because the optical path length is only a few centimeters here, shorter than the laser coherence length, it works very well in this setup.

When the free end of the piezo is displaced by half a wavelength, the pattern on the detector will change from maximum constructive interference to maximum destructive interference, and back. The intensity variations caused by these changes in interference are recorded by the photodetector. By adjusting the setup to be on the slope of the interference changes, a small signal is obtained that is linear in the displacement. If the displacement is a significant fraction of half the laser wavelength (which is 633 nm for the red laser diode module used in the setup), the signal becomes nonlinear and can even become periodic. Care should be exercised that the piezo displacement does not become too large.

The miniature optical setup is very stable against parasitic mechanical resonances, but its simplicity caused it to drift in and out of the region of maximum sensitivity once every few minutes. Therefore, the individual displacement measurement frequency sweeps had to recorded within one minute each. Because in this setup there is no absolute measurement of the displacement, the piezo displacement was normalized for the low-frequency response without series resistor. The sensitivity was not exactly the same every time the setup drifted in and out of the region of maximum sensitivity. Because not every individual displacement measurement frequency sweep was recorded the same sensitivity, the normalization had to be done independently for every measured curve. Other than this, no processing was performed on the measured data.

The frequency responses of the current through the piezo, the voltage across the piezo, and the displacement of the piezo were recorded with a computer-controlled HP 4194 A network analyzer. The setup is shown in Fig. 11. The current through the piezo was recorded by measuring the voltage drop that this current caused over a 0.2 Ω resistance in series with the piezo. This 0.2 Ω resistance was small enough not to affect the measurements. The voltage across the piezo was buffered and amplified by a 1 MΩ input Tektronix 7A26 preamplifier in a Tektronix 7904 A mainframe before it was sent to the network analyzer to prevent the network analyzer 50 Ω input from influencing the voltage across the piezo. The small

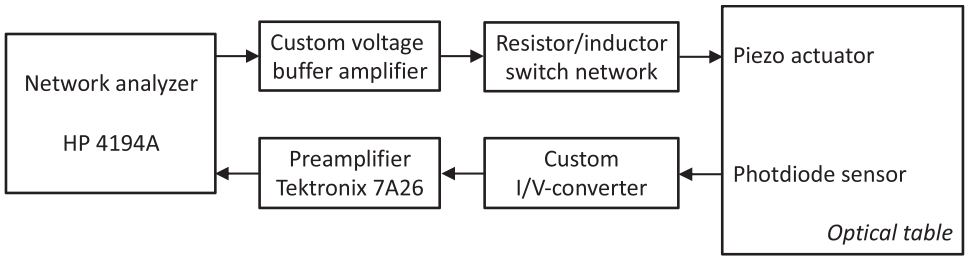

Fig. 11. Displacement transfer function measurement setup.

signal current of the photodetector signal was amplified by an in-house developed I/V-converter and then sent to the network analyzer. The piezo actuator was driven by an in-house developed 'hard voltage source' circuit that buffered and amplified the output voltage of the network analyzer. The output voltage of the source was 2.5 mV_{rms}, irrespective of the frequency. Different values of R_a could be switched in series with the piezo using a 10-fold dip-switch. The available R_a values were 0, 2, 5, 10, 22, 36, 50, 100, 300 and 1000 Ω. For the RL-compensation experiments, small inductors with negligible series resistance were soldered in series with R_a by hand. The inductance values used were 0, 100, 150, 220, 320, and 440 μH.

The piezo actuator used for the experiments was the Physik Instrumente P-820.20, a preloaded piezo actuator for light and medium loads. A preloaded piezo has a built-in restoring force, which assures that the brittle piezoceramic crystal will not break under moderate tensile forces. This improves the resistance of the piezo against cracking when used in frequency sweeps up to high frequencies. After all, the velocity, and hence the force on the piezo exerted by its own accelerating mass, increases linearly with frequency for a constant actuation voltage. The experiments performed for this paper drive the piezo actuator to very high frequency motion. A comparable, but not preloaded piezo actuator was actually damaged during early high frequency testing. The preload does not alter the theory presented above. In Table 2, the properties of the piezo are shown, as given by the manufacturer.

6. The resistively coupled piezo: experimental results

A full set of curves was recorded to illustrate and validate the theory presented in Sections 2–4. The magnitude of the current through the piezo was recorded for different values of R_a (Fig. 12), and the equation for $|i_{md}|$ given in Section 3 (Eq. 16) was fitted to the measured data to extract the piezo parameters R_m, C_m, L_m, and C_o as given before in Table 1. The theoretical fit using these data is shown for different values of R_a in Fig. 13. The parameters describing the piezo could in principle be determined from the data of Fig. 12 by curve fitting. However, Eq. (16) contains so many terms that it is difficult to make a curve fit procedure converge properly. Therefore, an iterative process of repeated educated guesses and plotting of curves was used instead. The starting values for this procedure were taken from the manufacturer's documentation that came with the piezo as given in Table 2.

Table 2
Properties of the P-820.20 preloaded piezo, given by the manufacturer [17].

Property	*Value*
Travel (0–100 V)	30 μm ± 20%
Large signal stiffness	7 N/μm ± 20%
Piezo mass (not the effective moving mass!)	11 g ± 5%
Resonance frequency	15 kHz ± 20%
Maximum pull force	10 N
Maximum push force	50 N
Electrical capacitance	0.7 μF ± 20%

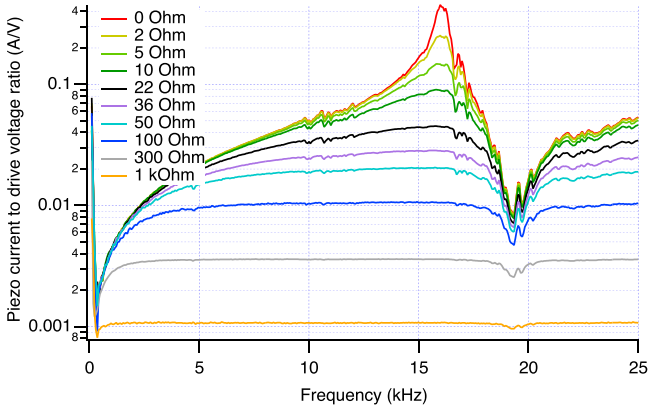

Fig. 12. Measured current through the piezo.

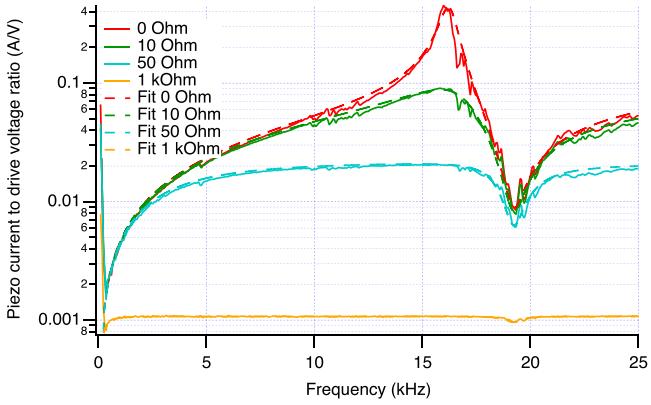

Fig. 13. Measured current through the piezo and theoretical fit.

The agreement between theory and current measurement experiment is extremely good, proving that the Butterworth–van Dyke model describes the electronic behavior of the piezo actuator to a very high degree.

In the next experiment, the magnitude of the voltage $|v_{piezo,md}|$ across the piezo was recorded for different values of R_a (Fig. 14). As the current through the piezo and R_a in series follows the theory, the same should be the case for the voltage, and indeed the fit is excellent (Fig. 15). Only with $R_a = 0\,\Omega$, there is a small resonance present. This reflects the small remaining output resistance of the 'hard' voltage source used to drive the piezo. But its effect is much smaller than even the R_a of just 2 Ω. No adjustments were made to the piezo model parameters to fit these curves.

The magnitude of the displacement $|d_{md}|$ of the piezo actuator was measured using the interferometer (Fig. 16). The amplitude in these figures has been calibrated to the static sensitivity of the piezo. The static sensitivity is found by noting that the piezo travels 30 μm

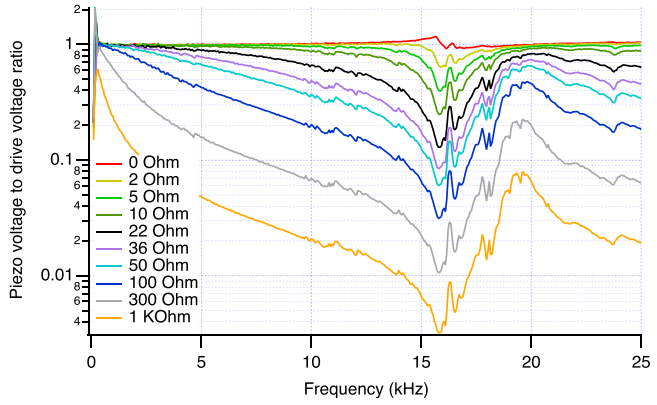

Fig. 14. Measured voltage across the piezo.

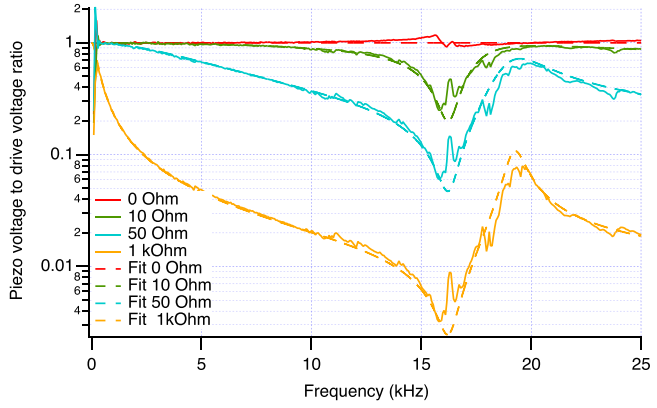

Fig. 15. Measured voltage across the piezo and theoretical fit.

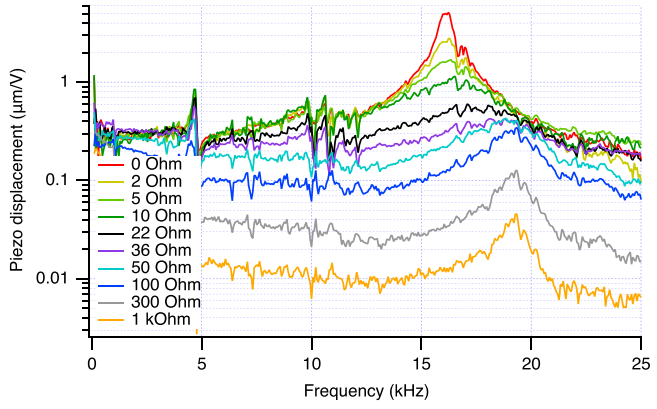

Fig. 16. Measured piezo displacement.

per 100 V actuation voltage as given by the manufacturer of the piezo (see Table 2). This results in 0.3 µm/V static sensitivity, accurate to within ± 20%. The agreement between theory and experiment shows that the displacement of the piezo with the integral of the mechanical current $|i_{mech,md}|$ is a good approach (Fig. 17). It should be noted that the theoretically found 'optimum' R_a, being $R_{a,mid} \cong 20\,\Omega$ is easily spotted in Fig. 13, and corresponds to the experimentally used value of $R_a = 22\,\Omega$. This also validates the new theory presented in Appendix A.

This is an important result. Because the primary resonance grows much faster if $R_a < R_{a,mid}$ than the anti-resonance if $R_a > R_{a,mid}$, it may

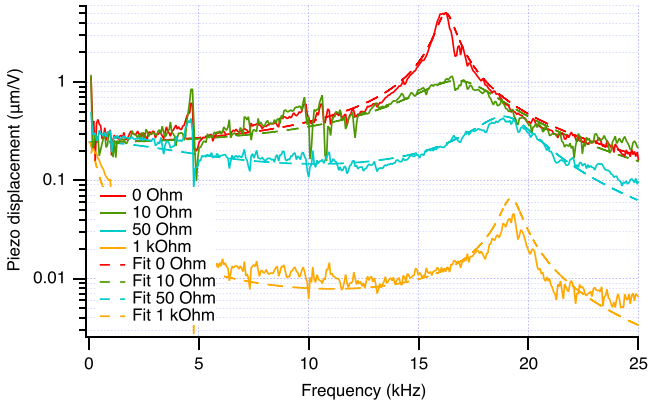

Fig. 17. Measured piezo displacement and theoretical fit.

be advisable to use some margin on $R_{a,mid}$ in practice. This results in a slightly larger recommended value of $R_{a,mid}$ for most applications. If the details of the resonant system are not important in their own right, but only a high damping of the piezo resonance is required, a series resistance R_a with a value of e.g. 50 Ω can be considered a good choice. This series resistance can be implemented as a stand-alone power resistor in series with a piezo driver with a low output impedance, but is already implemented in the output stage of some commercial high voltage amplifiers. Interestingly, Schitter et al. [20] also advocate the use of a 50 Ω resistance in series with the (completely different) piezo actuator that they use in an AFM (atomic force microscope) system. They attribute the effect to the low-pass filter formed by this resistor and the piezo capacitance, but in their frequency sweep figures the suppression of the primary resonance as per the above theory is very visible.

Note that in Fig. 16 a number of sharp, but much lower amplitude mechanical resonance peaks are visible around 5 kHz and 10 kHz. These peaks completely dominated the experiments when the setup was still using a proximity sensor. The proximity sensor is much more sensitive to lateral displacements than an interferometer. These peaks did not significantly change with the material (aluminum, granite or lead) of the optical table. It is therefore thought that these peaks represent mechanical (bending) resonances of the piezo housing. They are presumably not caused by the piezo crystal itself, as the quality factor Q of these peaks does not depend on R_a. Apart from these bending modes, additional noise is observed in the measured displacement curves, caused by three effects. To keep the added mass to a minimum, an only partially reflective piece of adhesive tape is used as the 'mirror' on the piezo as stated before. This lowers the available light intensity for interference significantly, but minimizes the excitation of the piezo bending modes. The amplitude of the displacement also has to be kept very small, due to the interferometric measurement. At the highest amplitude point of the resonance curve, the displacement should still be smaller than half the laser wavelength, or < 300 nm. The displacements in the measurements with the large series resistances are even smaller than those of the lowly damped measurements. This is caused by the low-pass filtering effect discussed in Section 2.

7. The RL-coupled piezo: experimental results

In the last set of frequency sweep experiments, the validity of the RL-compensation theory was investigated. These experiments were carried out immediately after those of Fig. 16 so that the system had no time to drift. In Fig. 18, the measured results are presented of the displacement magnitude $|d_{md,L}|$. The primary resonance with $R_a = 0\,\Omega$ is shown as a reference, in conjunction with several curves with the series resistance value closest to $R_{a,mid} \cong 20\,\Omega$, being $R_a = 22\,\Omega$. This

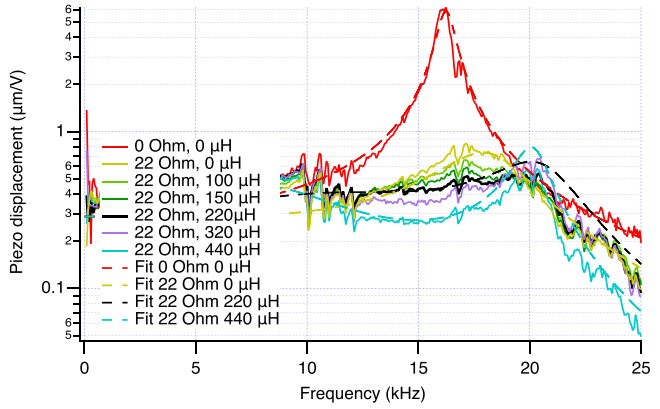

Fig. 18. Measured piezo displacement versus compensation inductance L_a and theoretical fit.

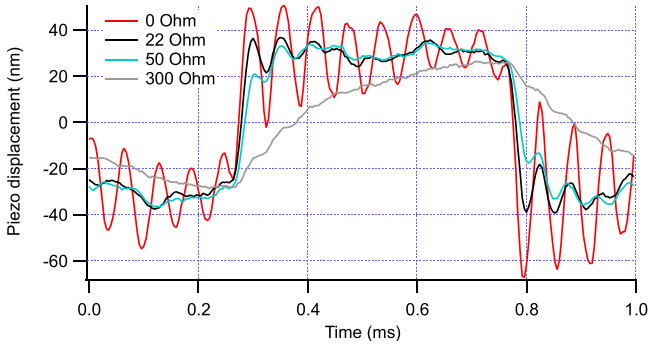

Fig. 20. Measured damping of the displacement step response ringing due to R-coupling.

resistance value was used with several values of L_a in series, resulting in a further flattening of the curve, and a shift of the remaining resonance towards the anti-resonance frequency. The optimal value of L_a that was experimentally found is 220 µH. At the midpoint frequency $\omega_{mid} = 2{\cdot}\pi{\cdot}17.5$ kHz between the primary resonance and the anti-resonance, the impedance of L_a is $\omega_{mid}L_a = 24\,\Omega$, which is indeed very close to $R_{a,mid}$.

It should be noted that the theoretical fits of the RL-compensation theory are less exact than those of the earlier measurements. This is caused by the fact that the compensation is much more sensitive to component values compared to the situation where only R_a is present. Some further tweaking of the values of $R_{a,mid}$ and L_a will possibly create a symmetrical 'saddle-like' double peak with very low amplitude in Fig. 18. The main reduction of the resonance amplitude however is caused by the choice of the proper R_a value. Indeed, the remaining peaking in the displacement without L_a is only a factor 2. If the mechanical damping R_m of a piezo actuator is lower than it is for the piezo used in this experiment, RL-compensation may be more beneficial, but at the same time, the sharper resonances will impose stricter requirements on the exact values of R_a and L_a.

8. Time domain measurements

The suppression of the resonance peak in the piezo displacement transfer functions (Figs. 16 and 18) is equivalent to the minimization of 'ringing' in the time domain. Experiments were performed with R- and RL-coupling to illustrate how the step response of the piezo displacement is improved by the suppression of the resonance peak.

The step response drive signal was a 1 kHz, 100 mV_{pp} square wave generated by a National Instruments USB-6211 data acquisition system that for this experiment replaced the network analyzer. To prevent damage to the piezo, which could be caused by the high-frequency energy of the square wave, a 30 kHz first order low pass filter was used in the piezo driver circuitry.

Electric and acoustic interference were rejected by placing the setup in a sound-proof Faraday cage and by running the piezo driver and photodiode circuits on batteries. The signal from the photodiode circuit was amplified using a Falco Systems RVPA-442 low noise voltage preamplifier. To improve the signal-to-noise ratio of the time domain measurements further, the step response was recorded 10,000x and averaged, thereby increasing the signal-to-noise ratio by $\sqrt{10{,}000} = 100$ times.

After the measurement was performed, the piezo on the optical table was turned in such a way that its light beam was no longer reflected onto the photodiode. The remaining electrical cross-talk was recorded in the same way as in the measurement itself and subtracted from the step response measurements. The setup is shown in Fig. 19.

The use of R- and RL- coupling indeed improves the damping of the piezo step response, as expected. This is shown in Figs. 20 and 21.

The step response for actuation with 0 Ω series resistance in Fig. 20 shows a high amplitude ringing that slowly damps out. This is consistent with the high resonance peak for the 0 Ω frequency response curve in Fig. 16. The case of optimal damping, 22 Ω, as calculated in Eq. (26), has a fast step response and much reduced ringing. However, the 50 Ω step response curve is almost as fast and has a lower maximum overshoot, so it may be more desirable for many applications. The step response with 300 Ω series resistance is much slower due to the pronounced low-pass filtering effect. In addition, the low pass filtered but relatively high Q ringing of the anti-resonance is slightly visible in the 300 Ω curve on top of the slow step response.

In Fig. 21, it can be seen that the introduction of the optimum value inductor for the case of RL-coupling hardly lowers the ringing compared to R-coupling alone. The effect is much smaller than the difference between 0 Ω and 22 Ω resistive damping. Also visible in Figs. 20 and 21 is a lower frequency resonance superimposed on the step response. This resonance is associated with the sharp parasitic resonance peak of the setup near 5 kHz that is also visible in Fig. 16.

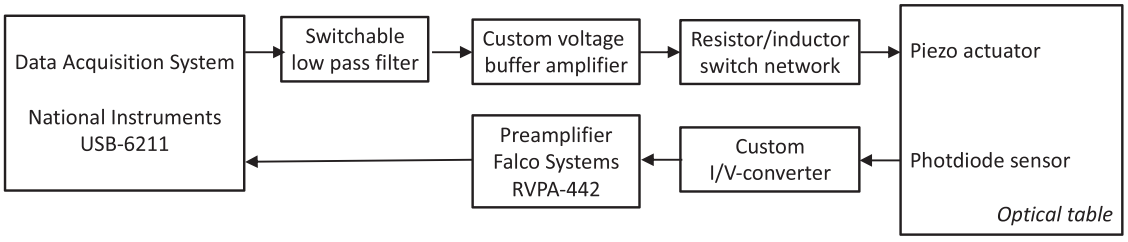

Fig. 19. Time domain measurement setup.

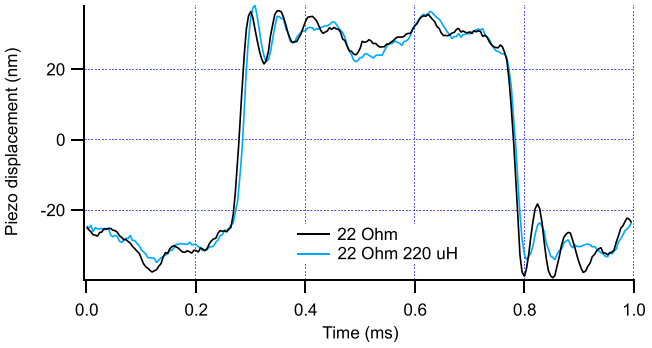

Fig. 21. The effect of RL-coupling on the measured displacement step response.

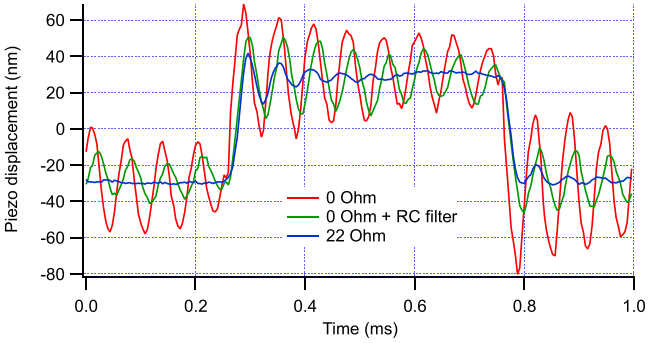

Fig. 22. Comparison of electronic damping and low-pass filtering the input signal.

Separate low-pass filtering of the input signal is not nearly as effective as electronic damping at the piezo, as theoretically discussed in Section 2. This is shown in the measurement of Fig. 22. The optimal resistance of 22 Ω together with the piezo capacitance of 0.67 μF forms an RC filter with a resonance frequency of −3 dB at 10.6 kHz that will lower the resonance amplitude even in the absence of electronic damping. An equivalent RC filter of 220 Ω and 68 nF (resonance frequency also 10.6 kHz) was added to the input signal circuitry (see Fig. 19) and the piezo driven without series resistance. In the case of separate low-pass filtering, the resonance amplitude is reduced somewhat, but the ringing time is still long, as expected.

9. Conclusions

Piezo actuators are very powerful and precise actuators, but are commonly plagued by electromechanical resonances that complicate their use. In this paper a comprehensive theory of electronic damping of piezo actuator resonances using resistor and resistor-inductor compensation is presented as seen purely from the electronic domain. The importance of associating the current through the 'mechanical' branch of the Butterworth–van Dyke model of a piezo with its velocity has been stressed, as this allows one to calculate the displacement of the piezo as a function of frequency using only calculations commonly used in the electronic domain. For a good description of the behavior of an actual piezo actuator, the mechanical damping of the piezo should not be neglected, but a simple theory (Section 2) is enough to illustrate the basic features of the piezo system with series resistance. Using these equations, we have found that an optimum series resistance can be calculated (Appendix A), which is ~20 Ω for PZT (Lead Zirconate Titanate) based piezo actuators, irrespective of the exact piezo used. The addition of the mechanical damping term in the theory results in more complex algebra to describe this damping. This inclusion of mechanical damping results in an almost exact fit to actual piezo actuator behavior.

For the experimental sections, a miniature optical table with interferometer setup was developed in-house to assess the mechanical displacement of the piezo under different electrical stimuli. The theory was illustrated by electronic measurements of the current through and the voltage across the piezo. The interferometer allowed a direct measurement of the displacement of the piezo as a function of frequency.

It has been found that the damping of the resonances of a piezo in both the electrical domain (current, voltage) and the mechanical domain (displacement) are very accurately described by the theory presented in this paper. If the series resistance between the voltage source and the piezo is low, a large mechanical resonance is observed at the primary resonance frequency of the piezo. If the series resistance is large, the resonance is observed at the slightly higher anti-resonance frequency, again with a high quality factor. In between lays the series resistance required for optimum damping. The fits of the theory to the experimentally obtained frequency response curves are excellent. This feat warrants a strong recommendation of the use of the Butterworth–van Dyke model in the way presented in this paper for the assessment of the mechanical response of piezo actuator systems. Step response measurements show that the damping features of the model in the frequency domain correlate to similar improvements in the time domain. Separate low-pass filtering of the input signal is not nearly as effective as direct electronic damping of the piezo.

It has been both theoretically and experimentally determined that a value of the series resistor that is less than the optimum value results in a much higher amplitude resonance than if the value of the series resistance is a bit too high. It is therefore recommended, in most cases, to use a series resistor of a value that is slightly larger than the calculated optimum, e.g. 50 Ω, if the piezo actuator is to be used with minimal electromechanical resonances. Compensation with the exactly optimal calculated resistance value, and resistor-inductor compensation, can only be recommended if a significant effort is spent on the exact electromechanical piezo actuator system and its mechanical response on a case-to-case basis.

Author statement

This work has been fully carried out by W. Merlijn van Spengen as the sole author.

Declaration of Competing Interest

The author declares that he has no known competing financial interests or personal relationships that could have appeared to influence the work reported in this paper.

Acknowledgments

The author would like to thank The Rijksdienst voor Ondernemend Nederland, part of the Dutch Ministry of Economic Affairs and Climate Policy, The Netherlands, for financial support in the WBSO framework under grant number SO20001246.

Appendix A. Derivation of the series resistance for optimal damping of the piezo

We can approximate the specific R_a for maximum damping, which we will call $R_{a,mid}$, by noting that this optimal R_a will be very close to the R_a required to bring the resonance peak frequency halfway in between the undamped primary resonance and the undamped anti-resonance frequency. For a treatment in the mechanical domain, see [12]. With the primary resonance being defined by the first term in the denominator of the calculation of the mechanical current $|i_{mech}|$, its frequency ω_{prim} is found by stating

$$1 - \omega_{prim}^2 C_m L_m = 0 \tag{24}$$

$$\omega_{prim}^2 = \frac{1}{C_m L_m} \tag{25}$$

Likewise, the undamped anti-resonance frequency ω_{anti} is found from the second term in the denominator as follows

$$C_o + C_m - \omega_{anti}^2 C_o C_m L_m = 0 \tag{26}$$

$$\omega_{anti}^2 = \frac{C_o + C_m}{C_o C_m L_m} \tag{27}$$

The R_a for maximum damping shifts the resonance frequency roughly halfway in between the two, to a frequency ω_{mid} given by

$$\omega_{mid} = \frac{\omega_{prim} + \omega_{anti}}{2} \tag{28}$$

By recognizing that $\omega_{prim} \approx \omega_{anti}$, we can also write

$$\omega_{mid}^2 \approx \frac{\omega_{prim}^2 + \omega_{anti}^2}{2} \tag{29}$$

By inserting the equations for the respective resonance frequencies, we find

$$\omega_{mid}^2 \approx \frac{2C_o + C_m}{2C_o C_m L_m} \tag{30}$$

To find the midpoint value of the resistance $R_{a,mid}$, we use the following procedure. We need an equation that gives the position of the resonance peak in the frequency spectrum as a function of R_a, after which we can set $\omega = \omega_{mid}$ to obtain $R_{a,mid}$. Note that at the resonance frequency the denominator of the mechanical current $|i_{mech}|$ is the lowest because the resonance amplitude described by this denominator is the highest there. So, to find the position of the resonance peak, we are looking for the minimum of

$$f(\omega) = (1 - \omega^2 C_m L_m)^2 + \omega^2 R_a^2 (C_o + C_m - \omega^2 C_o C_m L_m)^2 \tag{31}$$

At the top of the resonance, the derivative of this function is zero. To find the correct equation, we have to differentiate $f(\omega)$ and set this derivative to zero. By noting that

$$(f \cdot g)' = f'g + fg' \quad \text{and} \quad (f \cdot g \cdot h)' = f'gh + fg'h + fgh' \tag{32}$$

the differentiation of $f(\omega)$ can be carried out. We use $f = g = 1 - \omega^2 C_m L_m$ for the first part, and $f = \omega^2 R_a^2$, but $g = h = C_o + C_m - \omega^2 C_o C_m L_m$ for second part of the equation respectively, and obtain

$$f'(\omega) = 2 \cdot (-2\omega C_m L_m)(1 - \omega^2 C_m L_m) + 2\omega R_a^2 (C_o + C_m - \omega^2 C_o C_m L_m)^2 + 2 \cdot \omega^2 R_a^2 (-2\omega C_m C_o L_m)(C_o + C_m - \omega^2 C_o C_m L_m)$$

$$= -4\omega C_m L_m (1 - \omega^2 C_m L_m) + 2\omega R_a^2 (C_o + C_m - \omega^2 C_o C_m L_m)(C_o + C_m - 3\omega^2 C_o C_m L_m) = 0 \tag{33}$$

Hence R_a^2 is found to be

$$R_a^2 = \frac{2C_m L_m (1 - \omega^2 C_m L_m)}{(C_o + C_m - \omega^2 C_o C_m L_m)(C_o + C_m - 3\omega^2 C_o C_m L_m)} \tag{34}$$

By inserting

$$\omega^2 = \omega_{mid}^2 \approx \frac{2C_o + C_m}{2C_o C_m L_m} \tag{35}$$

and simplifying the resulting algebra, we find for the midpoint $R_a = R_{a,mid}$, for maximum damping

$$R_{a,mid}^2 = \frac{4C_m L_m}{C_o (4C_o + C_m)} \tag{36}$$

and finally

$$R_{a,mid} = 2\sqrt{\frac{C_m L_m}{C_o (4C_o + C_m)}} \tag{37}$$

References

[1] M.J. Rost, G.J.C. van Baarle, A.J. Katan, W.M. van Spengen, P. Schakel, W.A. van Loo, T.H. Oosterkamp, J.W.M. Frenken, Video-rate scanning probe control challenges: setting the stage for a microscopy revolution, Asian J. Control Vol. 11 (No. 2) (2009) 110.

[2] R.J. Matthys, Design of crystal oscillator circuits, in: J. Williams (Ed.), Analog Circuit Design, Butterworth-Heinemann, Newton, USA, 1991, p. 333.

[3] S.O.R. Moheimani, A.J. Fleming, Piezoelectric Transducers for Vibration Control and Damping, Chapter 4, Springer, London, UK, 2006.

[4] A.J. Moulson, J.M. Herbert, Electroceramics, second ed., John Wiley & Sons Ltd, Chichester, England, 2003.

[5] H.J.M.T.A. Adriaens, W.L. de Koning, R. Banning, Modeling piezoelectric actuators, IEEE ASME Trans. Mechatron. Vol. 5 (No. 4) (2000) 331.

[6] M.J. Hagmann, Analysis and equivalent circuit for accurate wideband calculations of the impedance for a piezoelectric transducer having loss, AIP Adv. 9 (2019) 085313.

[7] K.S. van Dyke, The piezo-electric resonator and its equivalent network, Proc. Inst. Radio Eng. Vol. 16 (No. 6) (1928) 742.

[8] D.S. Stutts, A simple example of the relationship between electromechanical coupling and measured impedance, Report to Mr. C. P. Mentesana at AlliedSignal Aerospace, 1995, retrieved from ⟨http://web.mst.edu/~piezo/MotorAnalysis/Impedancemodel/Imped-Mo.html⟩ on 26–4-2018.

[9] R. Queiros, P.S. Girao, A.C. Serra, Single-mode piezoelectric ultrasonic transducer equivalent circuit parameter calculations and optimization using experimental data, in: Proc. IMEKO TC4 Symposium, Volume II, Gdynia, Poland, 2005.

[10] Y. Fernandez-Afonso, O. Garcia-Zaldivar, F. Calderon-Pinar, Equivalent circuit for the characterization of the resonance mode in piezoelectric systems, J. Adv. Dielectr. Vol. 5 (No 4) (2015) 1550032-1.

[11] W. Sriratana, R. Murayama, L. Tanachaikhan, Synthesis and analysis of PZT using impedance method of reactance estimation, Adv. Mater. Chem. Phys. Vol. 3 (2013) 62.

[12] M. Prokic, Piezoelectric Transducers Modeling and Characterization, MPI, Le Locle, Switzerland, 2004.

[13] O. Thomas, J. Ducarne, J.-F. Deu, Performance of piezoelectric shunts for vibration reduction, Smart Mater. Struct. Vol. 21 (No. 1) (2012) 015008.

[14] A. Arnau (Ed.), Piezoelectric Transducers and Applications, second ed., Springer, Berlin, 2008Appendix 1.A.

[15] J. Kim, B.L. Grisso, J.K. Kim, D.S. Ha, D.J. Inman, Electrical modeling of piezoelectric ceramics for analysis and evaluation of sensory systems, in: Proc. IEEE Sensors Applications Symposium, Atlanta, GA, 2008, p. 122.

[16] G.J. Verbiest, D.J. van der Zalm, T.H. Oosterkamp, M.J. Rost, A subsurface add-on for standard atomic force microscopes, Rev. Sci. Instr. Vol. 86 (2015) 033704.

[17] Physik Instrumente datasheet of the P-820.20 preloaded piezo actuator, retrieved from ⟨https://static.physikinstrumente.com/fileadmin/user_upload/physik_instrumente/files/datasheets/P-820-Datasheet.pdf⟩ on 8-10-2020.

[18] A.J. Fleming, S.O.R. Moheimani, Sensorless vibration suppression and scan compensation for piezoelectric tube nanopositioners, IEEE Trans. Control Syst. Technol. Vol. 14 (No. 1) (2006) 33.

[19] R.M. Schmidt, G. Schitter, J. van Eijk, High Performance Mechatronics, Delft University Press, Delft, 2011.

[20] G. Schitter, P.J. Thurner, P.K. Hansma, Design and input-shaping control of a novel scanner for high-speed atomic force microscopy, Mechatronics Vol. 18 (2008) 282.

W. Merlijn van Spengen studied electrical engineering at the TU Eindhoven, The Netherlands, and earned a Ph.D. in applied science from the KU Leuven, Belgium, while staying at the independent microelectronics research center IMEC. Here he developed models for micro-scale adhesion and the effect of dielectric charging on MEMS (micro-electromechanical systems) switches. Back in the Netherlands, he continued his research first at Leiden University and later as an associate professor at TU Delft, working on MEMS reliability and electronic measurement technology. He has received the prestigious Veni and Vidi grants. Van Spengen is an experienced analog electronics design expert and founding director of the company Falco Systems. With his team at Falco Systems, he currently strives to provide the best laboratory preamplifiers and high voltage amplifiers for driving piezo actuators and MEMS devices.